



## Studies of the Confinement and the Toroidal Current Control in Heliotron J

OKADA Hiroyuki, SANO Fumimichi, KONDO Katsumi<sup>1)</sup>, MIZUUCHI Tohru, HANATANI Kiyoshi, NAKAMURA Yuji<sup>1)</sup>, NAGASAKI Kazunobu, KOBAYASHI Shinji, BESSHO Saka<sup>1)</sup>, NAKASUGA Masahiko<sup>1)</sup>, MANABE Yoshito<sup>1)</sup>, SHIDARA Hiroyuki<sup>1)</sup>, KAWAZOME Hayato<sup>1)</sup>, KANEKO Masashi<sup>1)</sup>, TAKAMIYA Tasho<sup>1)</sup>, OHNO Yoshinori<sup>1)</sup>, NISHIOKA Yusuke<sup>1)</sup>, YUKIMOTO Hidetoshi<sup>1)</sup>, TAKAHASHI Koichi<sup>1)</sup>, NISHIO Shigeru<sup>1)</sup>, YAMADA Masaki<sup>1)</sup>, NAKAZAWA Shingo<sup>1)</sup>, TSUBOI Shintaro<sup>1)</sup>, FUKAGAWA Yohei<sup>1)</sup>, OHASHI Keisuke<sup>1)</sup>, SUZUKI Yasuhiro<sup>1)</sup>, IJIRI Yoshiyuki, SENJU Tohru, YAGUCHI Keiji, TOSHI Kiyoshi, SAKAMOTO Kinzo, SHIBANO Masashi, TRIBALDOS Victor<sup>3)</sup>, KONOSHIMA Shigeru<sup>4)</sup>, WAKATANI Masahiro<sup>1)</sup> and OBIKI Tokuhiko<sup>5)</sup>

*Institute of Advanced Energy, Kyoto University, Uji 611-0011, Japan*

<sup>1)</sup>*Graduate School of Energy Science, Kyoto University, Uji 611-0011, Japan*

<sup>2)</sup>*Graduate School of Engineering, Hiroshima University, Hiroshima 739-8527, Japan*

<sup>3)</sup>*Laboratorio Nacional de Fusion, Asociacion EUROTOM-CIEMAT, Madrid 28040, Spain*

<sup>4)</sup>*Japan Atomic Energy Research Institute, Ibaraki 311-0193, Japan*

<sup>5)</sup>*Kyushu Institute of Information Sciences, Dazaifu, Fukuoka 818-0117, Japan*

(Received 12 May 2004 / Accepted 16 August 2004)

The plasma confinement properties of Heliotron J plasmas and the toroidal current are investigated. A plasma energy of 2.5 kJ has been achieved by 70 GHz–0.35 MW electron cyclotron heating (ECH). The energy confinement time is within the expected values as determined by the stellarator scaling law. In the high density region, however, better confinement plasmas are observed. The transition phenomena characterized by  $H\alpha$  signal drop are sometimes observed in such a region. The toroidal current generally affects plasma confinement since it generates a poloidal magnetic field. From this point of view, toroidal current control is studied in terms of field-component variation and electron cyclotron current drive. The zero current condition is found in the inner vertical field scan. Current control using the electron cyclotron wave is also demonstrated.

### Keywords:

plasma confinement, H-mode, bootstrap current, ECCD, Heliotron J

## 1. Introduction

Heliotron J is a flexible helical-axis heliotron that was designed and constructed at Kyoto University as part of an experiment to explore a new concept for the optimization of the helical-axis heliotron device [1,2]. The main characteristics of Heliotron J are the strongly modulated helical variation of its magnetic axis, the resultant reduction of the neoclassical  $1/\nu$  transport, the favorable MHD characteristics due to its edge magnetic well, and its operational capability of studying the island divertor as well as the helical divertor [3]. Selected device parameters are as follows: the major radius of the torus  $R = 1.2$  m, the minor radius of the plasma  $a = 0.1$ – $0.2$  m, the helical coil pole number  $L = 1$ , the pitch number  $M = 4$ , the pitch modulation  $\alpha = -0.4$ , the rotational transform  $\iota/2\pi = 0.3$ – $0.8$ , the edge well depth of 1.5%, and the magnetic field on the axis  $B \leq$

1.5 T. Two types of ECH system of 53.2 GHz and 70 GHz, and a neutral beam injection (NBI) system are installed as shown in Fig. 1.

For the first stage of the plasma experiment, ECH plasma production and heating studies were carried out using three 53.2-GHz gyrotrons. The microwave mode, the pulse width, and the maximum power were TE<sub>02</sub>, 40–50 ms, and 0.4 MW, respectively. As for the breakdown characteristics of Heliotron-J plasmas, it was found that there exists a relatively wide range of the setting magnetic field strengths as compared with that of Heliotron E [4]. The optimal heating condition was found to be in general agreement with case in which the second harmonic resonance layer could be located near the magnetic axis in the straight section of the torus. On the other hand, a highly efficient ECH was found to exist in the high magnetic field region of more than  $B(0) = 1.4$  T, where no

author's e-mail: okada@center.iae.kyoto-u.go.jp

This article is based on the invited talk at the 20th JSPF Annual Meeting (Mito, 2003).

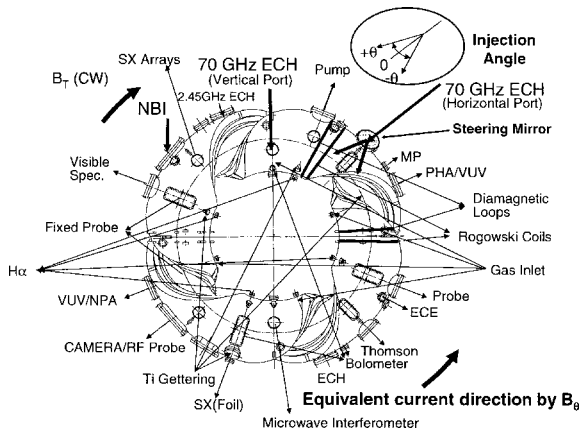


Fig. 1 Experimental setup of Heliotron J. A plasma is generated by the 70-GHz ECH from the horizontal port or the vertical port.

resonance layer for 53.2-GHz waves exists in the plasma core region. This heating mechanism remains to be studied in relation to the electron Bernstein wave heating using the edge fundamental resonance layer [5].

The other ECH system, a 70-GHz, 0.4-MW ECH system, was installed in Heliotron J in order to study the confinement relating to the localized heating of ECH as well as the magnetic field dependence. In the perpendicular injection scheme, the diameter of the injected beam (TEM<sub>00</sub> mode) is about 44 mm in e<sup>2</sup>-folding power at the magnetic axis position. A steering flat-mirror is used in the launching system as a final mirror to change the injection direction, and has a steering range of -15°/+30° and ±25° in the toroidal and poloidal directions, respectively. Definition of the steering angle is shown in Fig. 1. The ECCD experiment was made using this beam-launching system.

The magnetic field configuration of Heliotron J is generated by 6 sets of coils. They are a helical coil, main vertical coils, outer vertical coils, inner vertical coils, toroidal A coils, and toroidal B coils. The helical coil and the main vertical coils are connected serially. The magnetic configuration is then changed by controlling the ratio of the currents of five power supplies. The example of field variation is shown in Fig. 2 by changing the inner vertical coil current (*IV*) expressed by the ratio of the current to its maximum value. In this scan, primarily the bumpy component is changed. The rotational transform is also changed from 0.66 to 0.55; therefore, the shape of the outermost magnetic surface with 7 vertexes at *IV* = 72% becomes one with 6 vertexes at *IV* = -77%.

Global confinement properties mainly in the standard configuration (STD) [1] and the transition phenomena in the good confinement plasmas are described in Sec. 2 and 3. Control of the bootstrap current is one of the critical issues for Heliotron J design in order to maintain a magnetic field configuration in a good confinement property. The neoclassical toroidal current and the control of the toroidal current are investigated using the focused ECH beam. The results are mentioned in Sec. 4 and 5.

## 2. Confinement Properties of the ECH Plasmas

The second harmonic heating using focused 70-GHz ECH is performed for the more effective heating and the clearer experiment on the cyclotron condition. For the same power level of 0.35 MW, the stored energy of the 70-GHz ECH plasmas reached 2.5 kJ while the stored energy of the 53.2-GHz ECH plasmas was less than 1 kJ. In both cases, the stored energy increased with the density. Heating of the 70-GHz ECH system is effective below the X-mode cutoff density ( $3.0 \times 10^{19} \text{ m}^{-3}$ ). The energy dependence was investigated by changing the magnetic field strength, which also means the resonance position changes. The X-mode ECH beam is injected perpendicularly to the magnetic field from the horizontal port on the corner section [1], where grad *B* is steep along the major-radius direction as shown in Fig. 2. The plasma energy's dependence on magnetic field is shown in Fig. 3 (a). The plasma energy (*W<sub>p</sub>*) is estimated based on the diamagnetic loop signal at the straight section on the assumption that the stored energy is uniform along the toroidal direction. The plasma production and heating is effective in the range of 1.0 to 1.45 T, which is 20% of  $\Delta B/B_0$  where *B*<sub>0</sub> corresponds to the second harmonic resonance condition. Eighty percent of the maximum energy is maintained within 10% of  $\Delta B/B_0$ . This heating effectiveness in a wide *B* range is explained qualitatively by the ray-tracing calculation [6].

The confinement scaling of the ECH plasma in the density range of  $0.5\text{--}3.0 \times 10^{19} \text{ m}^{-3}$  agrees almost with the ISS95 [7] scaling as shown in Fig. 3 (b). The better confinement plasmas, whose confinement time is up to twice that of ISS95 scaling, are found under the high density condition [8]. The transition phenomena characterized with the drop of the H $\alpha$  line emission and the increase of the density and the energy as in the H-mode [9], are observed among the high density plasmas.

## 3. H-Mode Like Transition Phenomena

The time evolution of plasma parameters with an H-mode-like transition is shown in Fig. 4. At the beginning of the transition, the H $\alpha$  and *I<sub>s</sub>* at the SOL decrease, and the density and the energy then increase. A situation exists in which an oscillation of about six kHz is observed during the transition. In that case, equal oscillation is observed in the ECE signal, *I<sub>s</sub>*, and the density. The duration time of the transition is about 10 ms, which is comparable with the energy confinement time. The energy change rate is 0.1 MW at the maximum in the energy rise period after the beginning of the transition. The energy changes from 1 to 1.9 kJ during the transition with rapid density increase. A remarkable increase of radiation loss is not seen from the bolometer measurement; therefore, the density increase is caused by the improvement in confinement instead of by the influx of impurities from the outside of the plasma. The energy confinement time normalized by the value determined from ISS95 scaling increases from 1 to 1.7 during transition as

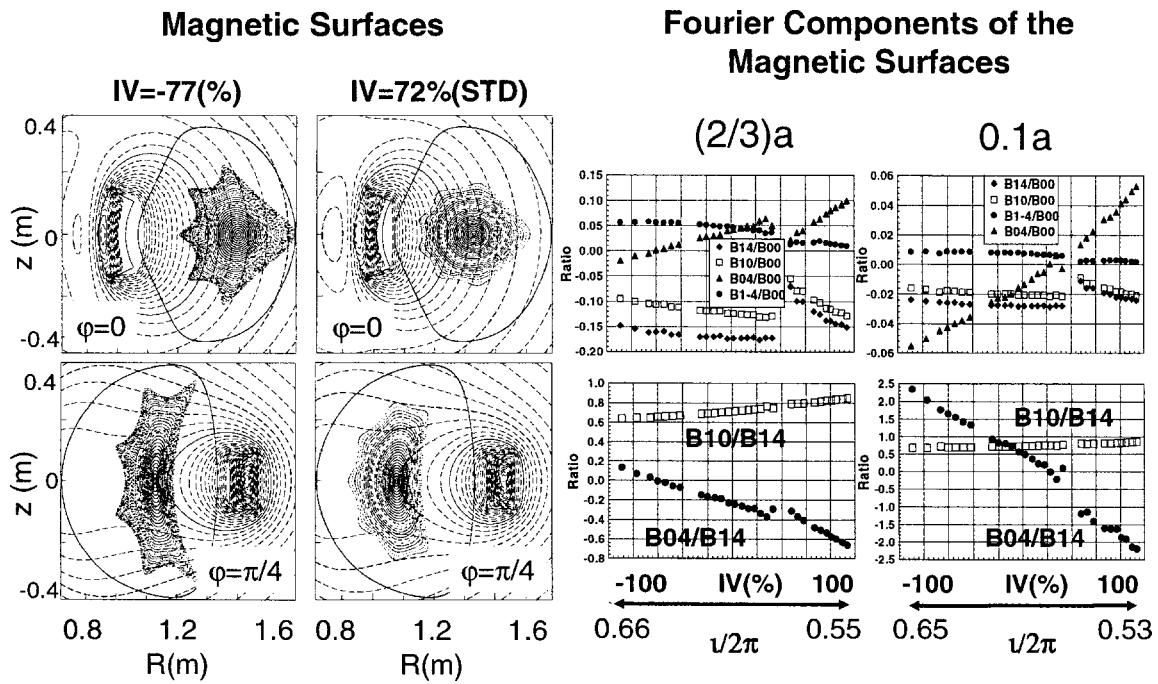


Fig. 2 Magnetic flux surfaces at various configurations, which are generated by changing the current of the inner vertical coil (Left side). Two cross sections at each configuration are described. In one the helical coil is located at  $z = 0$  on the inner side of the torus. The other is at the opposite location. The mod-B surfaces are also plotted by broken lines. The Fourier components of the major mode are plotted at the plasma's outer side ( $2a/3$ ) and near the center ( $0.1a$ ) on the right-top side. The ratio of the bumpy component to the helical component varies primarily at both positions.

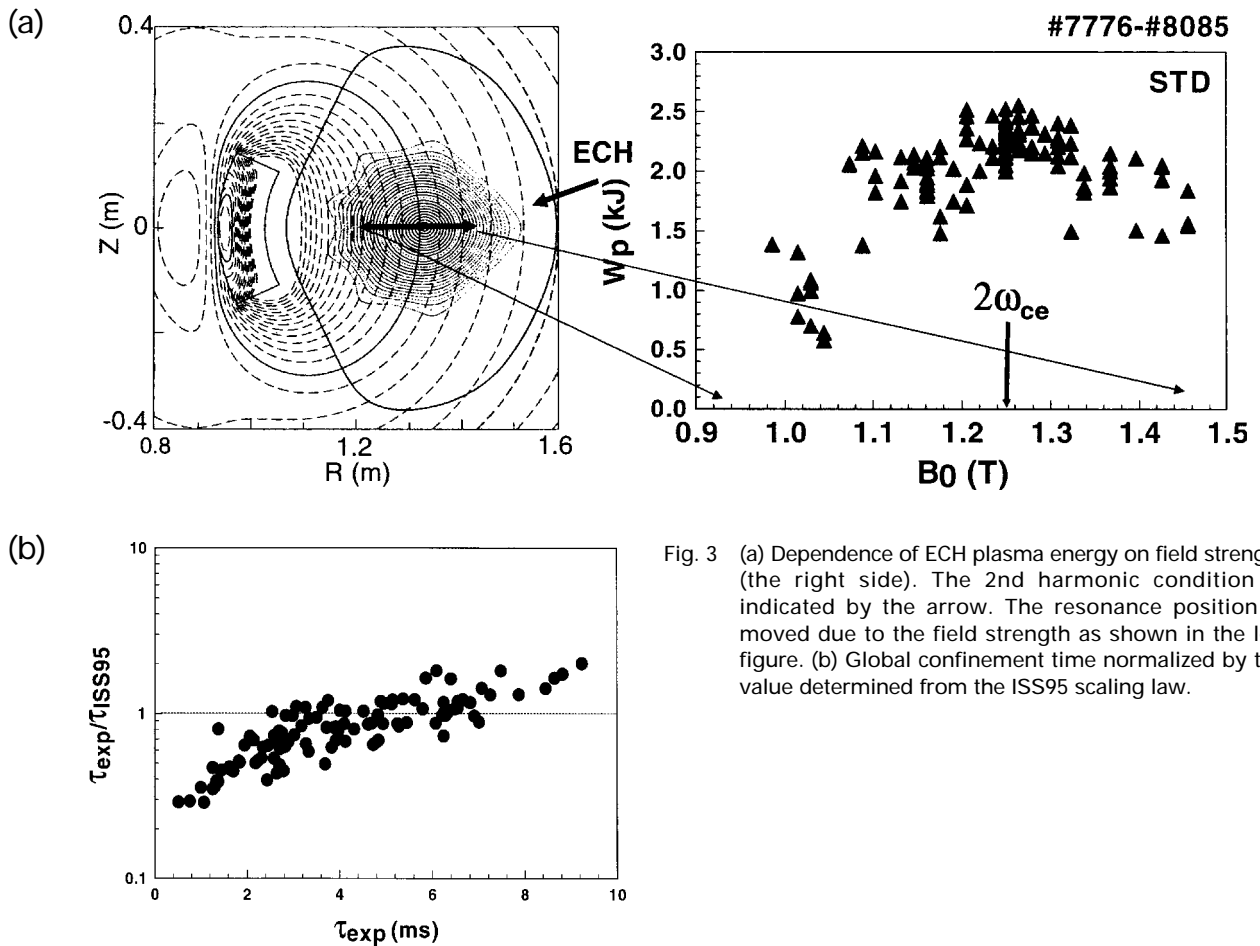


Fig. 3 (a) Dependence of ECH plasma energy on field strength (the right side). The 2nd harmonic condition is indicated by the arrow. The resonance position is moved due to the field strength as shown in the left figure. (b) Global confinement time normalized by the value determined from the ISS95 scaling law.

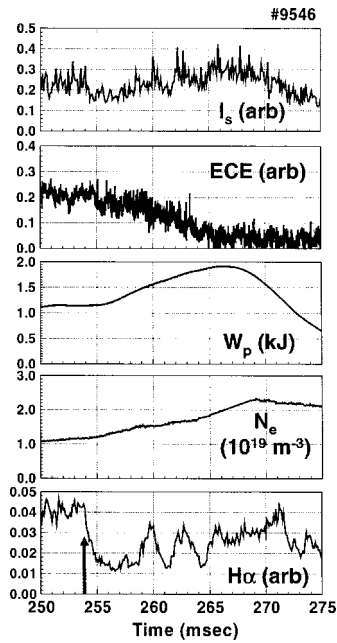


Fig. 4 Time evolution of the plasma parameters at the transition. The transition timing is indicated by the arrow.

shown in Fig. 5. These phenomena are terminated by the reduction of the temperature in the central region accompanied by an uncontrollable density increase resulting in radiation collapse or back-transition to the normal mode. The temperature decrease is considered to be due to the decrease of the absorbed power caused by the density cut-off of the ECH wave in the central region of the plasma.

Transition phenomenon is observed in the case in which the density or plasma energy is beyond a certain threshold value. Figure 6 shows the incidence of the transition phenomena in the relation of the injection power and the density. Transition occurs only in an energy of more than 1.0 kJ or in a density of more than  $1.1 \times 10^{19} \text{ m}^{-3}$ . The transition phenomenon does not occur under these values. Many experimental results of the H-mode have been reported since it was found in ASDEX. The threshold clearly depends on the incidence power [10]. However, power dependence is not recognized for Heliotron J plasma as shown in Fig. 6. For the H-modes in W7-AS which is one of the helical type devices, the threshold density dependence on input power is also different from that in tokamaks [11]. ELMy H-modes are obtained in a large parameter range. The operation condition of the H-mode in W7-AS is strongly related to the rotational transform. The dependence of the transition on rotational transform is also found in Heliotron J. An experimental study involving changing current ratios for five coil sets is now in progress.

#### 4. Bootstrap Current Control by the Field Configuration

The magnetic field for the confinement of Heliotron J plasma is formed only by the external coil current. Therefore, the internal toroidal current is not needed for the confinement

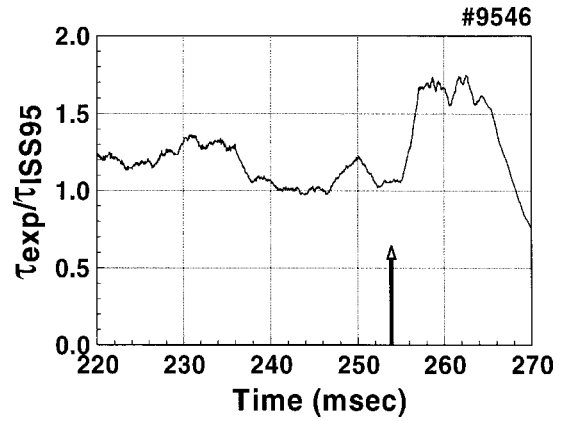


Fig. 5 The change of the confinement at the transition timing shown by the arrow.

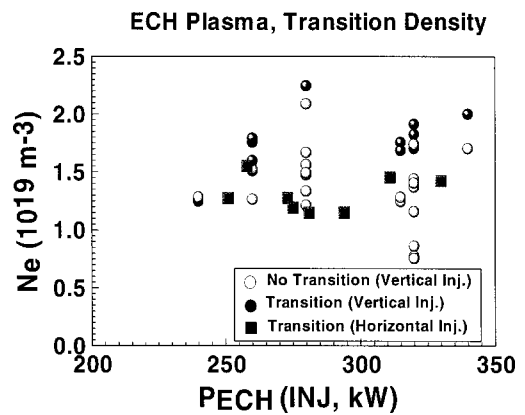


Fig. 6 Transition in the relation of the injection power and the line-averaged density.

field of Heliotron J plasmas. However, the toroidal current is produced by plasma itself due to the neoclassical effect. Helical devices are suitable for such study since they do not need toroidal current for generating the confinement field; therefore, small current is detectable. If the toroidal current is large enough to generate a low-mode rational surface in a plasma, it is possible that the confinement can be changed by the appearance of a large magnetic island in a low-shear device like Heliotron J. Control of the toroidal current is one of key issues in the Heliotron J plasma.

Plasma production and heating is performed by ECH using a 70 GHz-gyrotron having a power of less than 350 kW. The injection angle is perpendicular to the plasma axis in this STD configuration experiment. Therefore, no toroidal current is driven directly by the EC wave. The toroidal current ( $I_p$ ) is measured using Rogowski coils installed on the poloidal cross sections at two different toroidal angles as shown in Fig. 1. The two Rogowski coil signals are always identical within the range of experimental error.

The magnetic field where the current becomes its maximum of 2.2 kA is slightly different from the second harmonics resonance condition as shown in Fig. 7. The 2nd harmonic EC resonance in the case of the field strength of 1.16 T at the axis is located on the inner side of the torus as

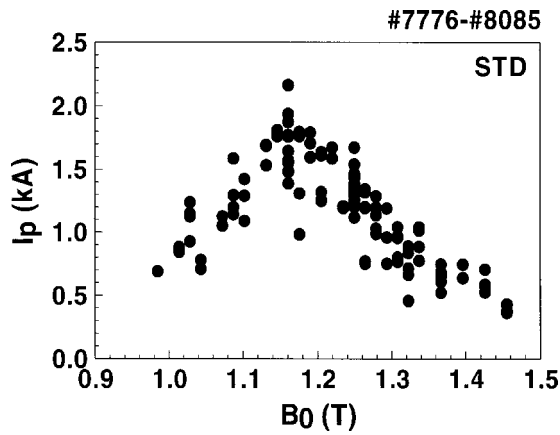


Fig. 7 Toroidal current dependence on field strength.

shown in Fig. 3 (a). It is considered that the better confinement for the trapped electrons on the inner side causes the shift from the 2nd harmonic resonance condition. The positive current indicates a counterclockwise current as seen from the top of the device. The current of 2.2 kA causes the change of the rotational transform at the plasma edge by less than 0.02; therefore, it does not significantly influence plasma confinement.

A change of the toroidal current is observed when the magnetic field configuration is controlled by one of the external coils, i.e., the inner vertical coil, with a density of about  $1 \times 10^{19} \text{ m}^{-3}$ . This control method mainly varies the bumpy component of the field line. The current decreases and is reversed finally when the inner vertical coil current decreases; that is, the configuration is changed from STD. The time evolutions of the toroidal current and the plasma energy are shown in Fig. 8 (a) and (b) for  $IV = -60\%$  and  $58\%$ , respectively. The current flows clockwise at  $IV = -60\%$ , whereas the current direction is counterclockwise at  $IV = 58\%$ . The maximum current value for each discharge is shown in Fig. 8 (c) in relation to  $IV$ . The toroidal current is suppressed to a negligible value near  $IV = 20\%$ . In addition, the current's maximum and minimum values are 1.5 kA and  $-1.2 \text{ kA}$ , respectively. The inner vertical field value at the STD configuration is indicated by the arrow. In this experiment the magnetic field strength is adjusted so that the second harmonic resonance (1.25 T) should be located at the plasma center. The measured energy is within 1.5–2.9 kJ except for the case of  $IV < -80\%$ . The current direction is reversed, maintaining the magnitude of the current when the confinement field is reversed by changing the coil current direction. These characteristics agree with those expected in the bootstrap current. The calculated values using the SPBSC code [12] are positive in the higher  $IV$  and negative in lower  $IV$ , as indicated by squares in Fig. 8 (c). The calculation of the bootstrap current in this code is based on the geometric factor  $G_{bs}$  for the  $1/\nu$  collisional regime by Shaing and Callen [13] and for the plateau collisional regime by Shaing *et al.* [14]. In this calculation, the effective ionic charge,  $Z_{\text{eff}}$ , is assumed to be unity and the temperature and density profiles are also assumed since there is no profiles data, yet. The

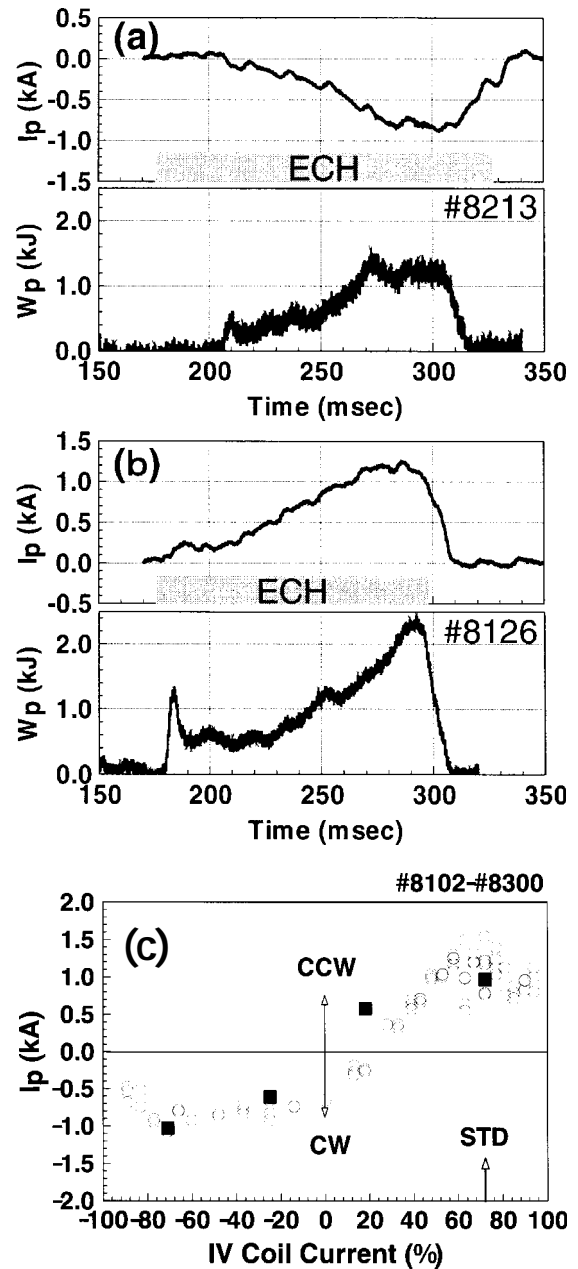


Fig. 8 (a) Time Evolution of plasma current and plasma energy at  $IV = -60\%$ . (b) Time Evolution of plasma current and plasma energy at  $IV = 58\%$ . (c) Change of the toroidal current due to the inner vertical coil current. The coil current is expressed by its percentage to the maximum coil current. The calculated values based on the neoclassical theory are also shown as solid squares using parameters:  $n_e = 1.5 \times 10^{19} (1-\rho^3) \text{ m}^{-3}$ ,  $T_e = 0.4 (1-\rho)^2 \text{ keV}$ ,  $T_i = 0.15 (1-\rho)^2 \text{ keV}$ ,  $Z_{\text{eff}} = 1$ , where  $\rho$  is the normalized minor radius.

change of the current direction is qualitatively explained by the neoclassical calculation, although the absolute value is changeable by factor of approximately 2 to accommodate the uncertainty of the profiles.

### 5. Toroidal Current Control by ECCD

The experiment regarding electron cyclotron current drive (ECCD) using a steering mirror system is performed in

order to certify the capability of the toroidal current control. This experiment is performed under the STD configuration. The injection angle of the ECH beam in the toroidal and poloidal directions can be changed by moving the steering mirror. In this experiment, the resonance position of the 2nd harmonic ECH wave is fixed at the plasma axis by adjusting the poloidal injection angle.

In the low density region of up to the  $0.5 \times 10^{19} \text{ m}^{-3}$ , the bootstrap current is about 0.3 kA. As a result, the maximum current is 1.2 kA and the minimum one is  $-0.7 \text{ kA}$ , respectively. The current after the subtraction of the offset by the bootstrap current is about 1 kA, generated equally in both toroidal directions as shown in Fig. 9. The null point appears near 3 degrees of the injection angle. The direction of the current generated by ECH is the opposite direction of the ECH beam as expected theoretically. The current drive efficiency is estimated to be 3 A/kW. When the magnetic field is reversed in order to confirm the ECCD, the current direction is unchanged against the injection angle. It flows again in the opposite direction to the beam.

In the case of a higher density of  $1.0 \times 10^{19} \text{ m}^{-3}$ , the current direction is not changed, as shown in Fig. 10, for any injection angle of the ECH beam. The bootstrap current is dominant as compared with the ECCD component in this case. However, the ECCD effect was observed even in this density region. The current values are larger in the negative injection angles than those in the positive angles. The dependence on the injection angle is almost the same as in the low density case, though the magnitude is slightly smaller in the high density case. The variation is 1.7 kA in the high density case and 1.9 kA in the low density case. Therefore, although the ECCD mechanism in the case of  $1.0 \times 10^{19} \text{ m}^{-3}$  is still active, its efficiency becomes smaller by about 10%.

## 6. Summary

As the result of study of ECH plasmas in Heliotron J, the good confinement has been achieved in the high density condition, which is about twice that of ISS95 scaling. The transition phenomena is found to be characterized by the drop of  $H\alpha$  and  $I_s$ , and the increase of density and energy. The threshold density is observed for the transition. A bootstrap current of up to 2.5 kA was observed in the ECH plasma of Heliotron J. Current control by a change of configuration using the inner vertical field coil was successfully carried out. The change of the current direction is qualitatively explained by numerical calculation based on the neoclassical theory. The bootstrap current was within the range of the neoclassical expectation. It was confirmed that the current was controllable by ECCD using a steering mirror system in the density range of  $0.5\text{--}1.0 \times 10^{19} \text{ m}^{-3}$ .

## Acknowledgements

This work was partially supported by the 21st Century COE Program of MEXT in Japan and by the Collaboration Program of the Laboratory for Complex Energy Processes, IAE, Kyoto University.

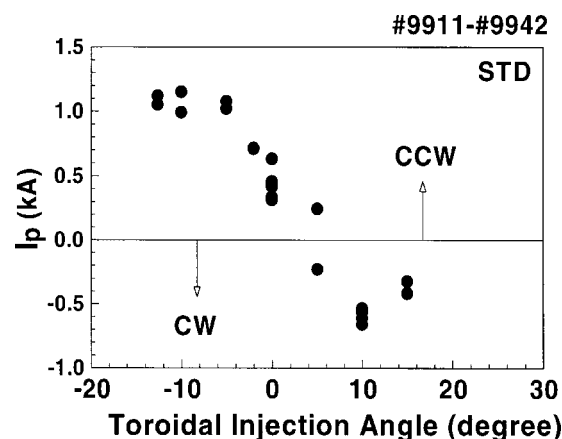


Fig. 9 Toroidal current change due to the toroidal injection angle of the ECH beam in the low density plasmas.

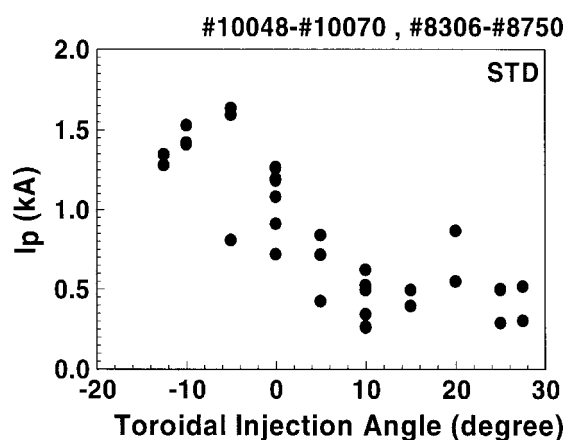


Fig. 10 Change of toroidal current due to the toroidal injection angle of the ECH beam in the high density plasmas.

## References

- [1] T. Obiki *et al.*, Plasma Phys. Cont. Fusion **42**, 1151 (2000).
- [2] M. Wakatani *et al.*, Nucl. Fusion **40**, 569-573 (2000).
- [3] F. Sano *et al.*, J. Plasma Fusion Res. Ser.3, 26-30 (1999).
- [4] T. Obiki *et al.*, Nucl. Fusion **41**, 833 (2001).
- [5] K. Nagasaki *et al.*, 13th Int. Stellarator Workshop, Canberra, P1-21N (2002), ANU web page: <http://www.rsphysse.anu.edu.au/admin/stellarator/proceedings.html>.
- [6] H. Shidara *et al.*, J. Plasma Fusion Res. **78**, 996 (2002).
- [7] U. Stroth *et al.*, Nucl. Fusion **36**, 1063 (1996).
- [8] T. Obiki *et al.*, Nucl. Fusion **44**, 47 (2004).
- [9] F. Sano *et al.*, J. Plasma Fusion Res. **79**, 1111 (2003).
- [10] M. Wakatani *et al.*, Nucl. Fusion **39**, 2175 (1999).
- [11] F. Wagner *et al.*, 19th IAEA-Conf. on Fusion Energy, Lyon, OV2-4 (2002).
- [12] K. Watanabe *et al.*, Nucl. Fusion **41**, 63 (2001).
- [13] K.C. Shaing and J.D. Callen, Phys. Fluids **26**, 3315 (1983).
- [14] K.C. Shaing *et al.*, Phys. Fluids **29**, 521 (1986).